

Claremont Colleges Scholarship @ Claremont

All HMC Faculty Publications and Research

HMC Faculty Scholarship

1-1-2009

Mathematical Model Creation for Cancer Chemo-Immuno-therapy

Lisette G. de Pillis
Harvey Mudd College

K Renee Fister
Murray State University

Weiqing Gu
Harvey Mudd College

Craig Collins
Murray State University

Michael Daub
Williams College

See next page for additional authors

Recommended Citation

L.G. de Pillis, K.Renee Fister, W. Gu, C. Collins, M. Daub, D. Gross, J. Moore, B. Preskill, "Mathematical Model Creation for Cancer Chemo-Immuno-therapy", *Computational and Mathematical Methods in Medicine*, Vol.10, No.3, 2009, pp. 165-184.

This Article is brought to you for free and open access by the HMC Faculty Scholarship at Scholarship @ Claremont. It has been accepted for inclusion in All HMC Faculty Publications and Research by an authorized administrator of Scholarship @ Claremont. For more information, please contact scholarship@cuc.claremont.edu.

Authors

Lisette G. de Pillis, K Renee Fister, Weiqing Gu, Craig Collins, Michael Daub, David Gross '08, James Moore '07, and Benjamin Preskill '09

Mathematical model creation for cancer chemo-immunotherapy¹

Lisette de Pillis^a, K. Renee Fister^{b*}, Weiqing Gu^a, Craig Collins^c, Michael Daub^d,
David Gross^e, James Moore^e and Benjamin Preskill^e

^aDepartment of Mathematics, Harvey Mudd College, Claremont, CA, USA; ^bDepartment of Mathematics, Murray State University, Murray, KY, USA; ^cMurray State University, Murray, KY, USA; ^dWilliams College, Williamstown, MA, USA; ^eHarvey Mudd College, Claremont, CA, USA

(Received 23 February 2008; final version received 13 May 2008)

One of the most challenging tasks in constructing a mathematical model of cancer treatment is the calculation of biological parameters from empirical data. This task becomes increasingly difficult if a model involves several cell populations and treatment modalities. A sophisticated model constructed by de Pillis *et al.*, *Mixed immunotherapy and chemotherapy of tumours: Modelling, applications and biological interpretations*, J. Theor. Biol. 238 (2006), pp. 841–862; involves tumour cells, specific and non-specific immune cells (natural killer (NK) cells, CD8⁺T cells and other lymphocytes) and employs chemotherapy and two types of immunotherapy (IL-2 supplementation and CD8⁺T-cell infusion) as treatment modalities. Despite the overall success of the aforementioned model, the problem of illustrating the effects of IL-2 on a growing tumour remains open. In this paper, we update the model of de Pillis *et al.* and then carefully identify appropriate values for the parameters of the new model according to recent empirical data. We determine new NK and tumour antigen-activated CD8⁺T-cell count equilibrium values; we complete IL-2 dynamics; and we modify the model in de Pillis *et al.* to allow for endogenous IL-2 production, IL-2-stimulated NK cell proliferation and IL-2-dependent CD8⁺T-cell self-regulations. Finally, we show that the potential patient-specific efficacy of immunotherapy may be dependent on experimentally determinable parameters.

Keywords: immune system model; cancer model; parameter estimation; mixed-immuno-chemo-therapy; immunotherapy; chemotherapy

AMS Subject Classification: 34A34; 46N10; 46N60

1. Introduction

The role of the immune system in the elimination of cancerous tissue is not fully understood. By constructing models of tumour–immune interaction founded on empirical data, it may be possible to enhance our understanding of the effects of immune modulation. Several papers have examined mathematical models of tumour–immune interactions in depth, including [2,3,7,8,10–13,24,27,29,34,36,38] to name a few. As explained in de Pillis *et al.* [12], the immune component is fundamental to understanding the growth and decay of a tumour, and if immunotherapy is to be used effectively in a clinical setting, its dynamic interactions with chemotherapy and the tumour itself must be understood.

*Corresponding author. Email: renee.fister@murraystate.edu

In particular, the dynamics and properties of both IL-2 and tumour antigen-activated CD8⁺T cells are continuing to be explored [32,41]. Indeed, only recently have techniques been developed to capture T-cell kinetics with detailed resolution [4]. Consequently, mathematical models of immune–tumour interactions must undergo updates with the latest research. As a more thorough understanding of the molecular processes is obtained, the mechanisms, rates and magnitudes of the interactions are revised appropriately.

In de Pillis *et al.* [12], the authors model tumour growth in terms of a total cell count by including the influence of several immune cell effector subpopulations, namely tumour antigen-activated CD8⁺T cells, natural killer (NK) cells and total circulating lymphocytes, in addition to the concentrations of IL-2 and chemotherapy drug in the bloodstream. This approach expands upon other models such as those investigated by Kirschner and Panetta [24], who considered a model based upon a total tumour cell population, an effector cell population and the concentration of IL-2 within the tumour compartment.

The model of de Pillis *et al.* [12] incorporates four types of action: natural growth, natural decay, mediated death and recruitment. Each term represents a population growing by reproduction, dying due to natural elimination, being killed by another population or drug or being recruited through a chain of immune reactions consequent to the presence of a cancer cell. Every term in the system of ordinary differential equations (ODEs) from the de Pillis *et al.* [12] model represents a single action. The authors also include the following assumptions:

- (1) the tumour grows logistically in the absence of growth-inhibiting factors;
- (2) endogenous IL-2 production is not included; and
- (3) the specific action of all lymphocytes beyond activated CD8⁺T cells and NK cells can be neglected.

The model we present similarly tracks the three immune populations, one tumour population and plasma concentrations of chemotherapy drug and IL-2. However, the action of immune cell subpopulations and chemicals in circulation (e.g. IL-2, chemotherapy drugs) necessarily depend on local concentration, not absolute number. We therefore elect to measure all state variables except the tumour cell count in terms of blood concentrations, which we assume are constant throughout the bloodstream. Furthermore, we investigate the kinetics of IL-2 and immune cell subpopulations, include endogenous IL-2 production and consider several biological IL-2 interactions, as discussed in Abbas *et al.* [1]. We also update the NK cell dynamics to allow for IL-2-stimulated NK cell proliferation, as indicated in Abbas *et al.* ([1]; p. 265). Although IL-2 does not bind as strongly to NK cells as it does to CD8⁺T cells, due to different IL-2 receptor subtypes, because of the super-physiological levels of IL-2 present during exogenous supplementation, the NK–IL-2 interaction changes the resulting dynamics [1]. Moreover, Abbas *et al.* [1] make clear that all types of T cells produce IL-2. If the model is to be applicable in the absence of IL-2 supplementation, baseline endogenous IL-2 production must be taken into account. Indeed, in untreated cancer patients, plasma IL-2 levels can reach the mid-saturation point for IL-2-stimulated CD8⁺T-cell deactivation and this effect is important in modelling the kinetics of T-cell populations [1,35]. Furthermore, Abbas *et al.* [1] discuss the self-regulation of CD8⁺T cells by helper CD4⁺T cells, another type of lymphocyte. This interaction is complex, as it is IL-2-dependent and only occurs when CD8⁺T cells become large in number. We include this interaction in our expansion of the IL-2 kinetics; without it, the self-reinforcing behaviour of CD8⁺T cells and IL-2 cause unphysiological behaviour in the form of unbounded CD8⁺T-cell production. By including the dynamic regulation of this immune cell subpopulation by IL-2, we are able to construct a model that comprises the proven efficacy of IL-2 when combined with CD8⁺T-cell infusion.

2. The model

In our update to the de Pillis *et al.* [12] model, we set out to include endogenous IL-2 production by CD4⁺ and CD8⁺T cells, account for IL-2-stimulated NK cell proliferation, capture IL-2 saturation with Michaelis–Menten dynamics and simplify certain parts of the model to allow for eventual optimal control analysis. We additionally altered and justified parameter values, inserted new parameters and modified state variable definitions.

Our first change was to alter the units of our state variables. Most of our sources, including Hellerstein *et al.* [20], Meropol *et al.* [30] and Dunne *et al.* [16], listed concentrations of immune cells as opposed to absolute quantities and we therefore found concentrations easier to work with in our model. We also stipulated that M represent a specific chemotherapy drug, doxorubicin, to allow for more precise parameter determination. Thus, we define

$T(t)$, the total tumour cell population;

$N(t)$, the concentration (cells/l) of NK cells per litre of blood;

$L(t)$, the concentration (cells/l) of CD8⁺T-cells per litre of blood;

$C(t)$, the concentration (cells/l) of lymphocytes per litre of blood, not including NK cells and CD8⁺T-cells;

$M(t)$, the concentration (mg/l) of chemotherapy drug per litre of blood;

$I(t)$, the concentration (IU/l) of IL-2 per litre of blood;

$v_L(t)$, the number of tumour-activated CD8⁺T cells injected per day per litre of blood volume (in cells/l per day);

$v_M(t)$, the amount of doxorubicin injected per day per litre of body volume (in mg/l per day); and

$v_I(t)$, the amount of IL-2 injected per day per litre of body volume (in IU/l per day).

The ODEs of our model are stated below. See Table 1 for an explanation of the terms. For a more in-depth justification of the terms taken from the their model, see de Pillis *et al.* [12]:

$$\frac{dT}{dt} = aT(1 - bT) - cNT - DT - K_T(1 - e^{-\delta_T M})T, \quad (1)$$

$$\frac{dN}{dt} = f\left(\frac{e}{f}C - N\right) - pNT + \frac{p_N NI}{g_N + I} - K_N(1 - e^{-\delta_N M})N, \quad (2)$$

$$\begin{aligned} \frac{dL}{dt} = & \frac{\theta mL}{\theta + I} + j\frac{T}{k + T}L - qLT + (r_1N + r_2C)T - \frac{uL^2CI}{\kappa + I} \\ & - K_L(1 - e^{-\delta_L M})L + \frac{p_I LI}{g_I + I} + v_L(t), \end{aligned} \quad (3)$$

$$\frac{dC}{dt} = \beta\left(\frac{\alpha}{\beta} - C\right) - K_C(1 - e^{-\delta_C M})C, \quad (4)$$

$$\frac{dM}{dt} = -\gamma M + v_M(t), \quad (5)$$

$$\frac{dI}{dt} = -\mu_I I + \phi C + \frac{\omega LI}{\zeta + I} + v_I(t), \quad (6)$$

where

$$D = d\frac{(L/T)^l}{s + (L/T)^l}. \quad (7)$$

Table 1. Equation descriptions.

Equation	Term	Description	Source
dT/dt	$aT(1 - bT)$	Logistic tumour growth	[12]
	$-cNT$	NK-induced tumour death	[12]
	$-DT$	CD8 ⁺ T cell-induced tumour death	[12]
	$-K_T(1 - e^{-\delta_r M})T$	Chemotherapy-induced tumour death	[12,18]
dN/dt	eC	Production of NK cells from circulating lymphocytes	[12]
	$-fN$	NK turnover	[12]
	$-pNT$	NK death by exhaustion of tumour-killing resources	[12]
	$(p_N NI/g_N + I)$	Stimulatory effect of IL-2 on NK cells	[12]
dL/dt	$-K_N(1 - e^{-\delta_n M})N$	Death of NK cells due to medicine toxicity	[12,18]
	$(-m\theta L/\theta + I)$	CD8 ⁺ T-cell turnover	[1,12]
	$-qLT$	CD8 ⁺ T-cell death by exhaustion of tumour-killing resources	[12,27]
	$r_1 NT$	CD8 ⁺ T-cell stimulation by NK-lysed tumour cell debris	[12]
	$r_2 CT$	Activation of native CD8 ⁺ T cells in the general lymphocyte population	[12]
	$(p_I LI/g_I + I)$	Stimulator effect of IL-2 on CD8 ⁺ T cells	[12,24]
	$(-uL^2 C/\kappa + I)$	Breakdown of surplus CD8 ⁺ T cells In the presence of IL-2	[1,12]
	$(jTL/k + T)$	CD8 ⁺ T-cell stimulation by CD8 ⁺ T cell-lysed tumour cell debris	[27]
	$-K_L(1 - e^{-\delta_t M})L$	Death of CD8 ⁺ T cells due to medicine toxicity	[12,18]
	dC/dt	α	Lymphocyte synthesis in bone marrow
$-\beta C$		Lymphocyte turnover	[12]
$-K_C(1 - e^{-\delta_c M})C$		Death of lymphocytes due to medicine toxicity	[12,18]
dM/dt	$-\gamma M$	Excretion and elimination of medicine toxicity	[12]
dI/dt	$-\mu_I I$	IL-2 turnover	[12]
	ϕC	Production of IL-2 due to naive CD8 ⁺ T cells and CD4 ⁺ T cells	[1]
	$(\omega LI/\zeta + I)$	Production of IL-2 from activated CD8 ⁺ T cells	[24]

In Equation (1), the tumour kinetics have been left largely unchanged in form. Our only modification involved adding a coefficient δ_r on M in the exponential kill term. This allows us more accurately to fit the model to data for doxorubicin and, in particular, avoids improper use of units.

In Equation (2), the NK equation has undergone two important changes. The recruitment term $gT^2N/(h + T^2)$ from the de Pillis *et al.* [12] model has been removed due to its observed insignificance within the context of the model, as evidenced by computer simulations and due to the additional complexity of the dynamics it introduces. We have added an IL-2-induced NK cell proliferation term, $p_N NI/(g_N + I)$. NK cells express the IL-2R β_{γ_c} IL-2 receptor and IL-2 binding stimulates NK cell proliferation [1]. Although, the enzyme dissociation constant k_d for this binding is sufficiently large that IL-2-stimulated NK cell proliferation is minimal in healthy individuals, it has been shown that additional IL-2 can more than double the NK cell population [30]. Consequently, in the presence of elevated serum IL-2, as occurs in cancer or during immunotherapy, this interaction may be important [16,35]. The first term in the NK equation represents baseline NK cell production from circulating lymphocytes, while the second models the natural death of the cells. We have chosen to write the term with the constant f as a multiplier to

highlight the fact that the constant elf , which denotes the baseline fraction of circulating lymphocytes that are NK cells, is particularly well known [1]. We added a coefficient δ_N on the exponential chemotherapy kill term for the same reasons we added δ_T .

Since the turnover rate of activated CD8⁺T cells is inhibited by IL-2, in Equation (3), we changed the term $-mL$ to $\theta mL/(\theta + I)$, [1]. That is, with increasing concentrations of IL-2 past a certain threshold, activated CD8⁺T-cell turnover is decreased. The θ in the numerator exists to preserve the original meaning of m . We then dramatically simplified the activated CD8⁺T-cell recruitment term, originally $jD^2T^2L/(k + D^2T^2)$, into the term $jTL/(k + T)$. Simulations of the de Pillis *et al.* [12] model indicated that the reaction-time delay introduced by the exponent on T did not offer sufficiently different results to justify the increased complexity of the model. Moreover, we observed that Kuznetsov *et al.* [27] use an effector recruitment term of same form as our modification. A significant alteration was made to the term originally $-uNL^2$. From Abbas *et al.* [1], we noted that the deactivation of CD8⁺T cells occurs through a pathway that requires IL-2 and the action of CD4⁺T cells (in circulating lymphocytes,) but not NK cells. Moreover, it occurs only at high concentrations of activated CD8⁺T cells. Consequently, we chose to alter the term $-uNL^2$ by removing the dependence on N , adding Michaelis–Menten dynamics in IL-2 and including factors of L^2 and C . Because 50–60% of the total lymphocytes in the blood are CD4⁺T cells, and because we have already removed NK cells (10% of total lymphocytes) and CD8⁺T cells (a negligible fraction of total lymphocytes) from C , we can approximate the concentration of CD4⁺T cells in the blood by ηC , where η is a constant absorbed into u ([1]; p. 19; [39]). Finally, we also included the same coefficient addition to the exponential chemotherapy kill term, using this time δ_L .

We did not significantly alter the circulating lymphocyte Equation (4). Our two minor modifications were to use a multiplier β that comes from the first and second terms (which represent creation and elimination of circulating lymphocytes, respectively) to emphasize the fact that α/β , the steady-state population of circulating lymphocytes is known ([1]; p. 17). We also added the exponential chemotherapy kill term in the form of δ_C .

In Equation (5), the terms remain the same.

In Equation (6), we added a term representing the constant rate of creation of IL-2 from circulating lymphocytes (specifically CD4⁺T cells and, to a lesser extent, naive CD8⁺T cells) in the form of ϕC and a Michaelis–Menten term in IL-2, $\omega LI/(\zeta + I)$, representing the production of IL-2 from activated CD8⁺T cells, which is inhibited in a concentration-dependent fashion by IL-2 ([1]; pp. 264–265).

3. The parameters

Careful determination of parameters is necessary for a complete model. We searched the available peer-reviewed literature for *in vivo* and *in vitro* studies measuring rates or steady-state quantities that factor into the model. Below, we explain our sources for each parameter and Tables 2 and 3 provide quick references for the parameter values and their significance within the model.

3.1 Equilibrium states

Before discussing the derivation of parameters, we determine from biological data reasonable equilibrium values for a no-tumour condition and a detectable tumour condition. These no-tumour and high-tumour state values are useful for extrapolating numerical quantities for several model parameters. Data for the detectable tumour state

Table 2. Parameter descriptions.

Equation	Parameter	Description
dT/dt	a	Growth rate of tumour
	b	Inverse of carrying capacity
	c	Rate of NK-induced tumour death
	K_T	Rate of chemotherapy-induced tumour death
	δ_T	Medicine efficacy coefficient
dN/dt	ef	Ratio of NK cell synthesis rate with turnover rate
	f	Rate of NK cell turnover
	P	Rate of NK cell death due to tumour interaction
	p_N	Rate of IL-2 induced NK cell proliferation
	g_N	Concentration of IL-2 for half-maximal NK cell proliferation
	K_N	Rate of NK depletion from medicine toxicity
	δ_N	Medicine toxicity coefficient
dL/dt	m	Rate of activated CD8 ⁺ T-cell turnover
	θ	Concentration of IL-2 to halve CD8 ⁺ T-cell turnover
	q	Rate of CD8 ⁺ T-cell death due to tumour interaction
	r_1	Rate of NK-lysed tumour cell debris activation of CD8 ⁺ T cells
	r_2	Rate of CD8 production from circulating lymphocytes
	p_I	Rate of IL-2 induced CD8 ⁺ T-cell activation
	g_I	Concentration of IL-2 for half-maximal CD8 ⁺ T-cell activation
	u	CD8 ⁺ T-cell self-limitation feedback coefficient
	κ	Concentration of IL-2 to halve magnitude of CD8 ⁺ T-cell self-regulation
	j	Rate of CD8 ⁺ T-lysed tumour cell debris activation of CD8 ⁺ T cells
	k	Tumour size for half-maximal CD8 ⁺ T-lysed debris CD8 ⁺ T activation
	K_L	Rate of CD8 ⁺ T depletion from medicine toxicity
	δ_L	Medicine toxicity coefficient
dC/dt	α/β	Ratio of rate of circulating lymphocyte production to turnover rate
	β	Rate of lymphocyte turnover
	K_C	Rate of lymphocyte depletion from medicine toxicity
	δ_C	Medicine toxicity coefficient
dM/dt	γ	Rate of excretion and elimination of doxorubicin
dI/dt	μ_I	Rate of excretion and elimination of IL-2
	ω	Rate of IL-2 production from CD8 ⁺ T cells
	ϕ	Rate of IL-2 production from CD4 ⁺ /naive CD8 ⁺ T cells
	ζ	Concentration of IL-2 for half-maximal CD8 ⁺ T-cell IL-2 production
D	d	Immune system strength coefficient
	l	Immune strength scaling coefficient
	s	Value of $(L/T)^l$ necessary for half-maximal CD8 ⁺ T-cell toxicity

can be taken, for example, from a situation in which an avascular tumour is at the size where the rates of nutrient usage and diffusion become equal.

The first equilibrium point we will call the *no-tumour equilibrium*, in which

$$T=0, N=\frac{e\alpha}{f\beta}=2.5\times 10^8, L=2.526\times 10^4, C=\frac{\alpha}{\beta}=2.25\times 10^9, M=0, I=48.9273. \quad (8)$$

Here T and M are defined to be equal to zero. The algebraic expressions for N and C follow from setting $T = M = 0$ in Equations (2) and (4), and the numerical values are derived below (see the explanations of ef in Section 3.3 and α/β in Section 3.5). Our value for I is obtained from Oditura *et al.* [35], who note that healthy control subjects had average serum IL-2 levels of $I = 2.99 \text{ pg/ml} = 48.9273 \text{ IU/l}$, where we have converted to IU using the

Table 3. Parameter values.

ODE	Parameter	Value	Units	Source
dT/dt	a	4.31×10^{-1}	Day ⁻¹	[12,14]
	b	1.02×10^{-9}	Cells ⁻¹	[12–14]
	c	2.9077×10^{-13}	l/cells ⁻¹ per day ⁻¹	[12–15]
	K_T	9×10^{-1}	Day ⁻¹	[12]
	δ_T	1.8328	l/mg ⁻¹	[18]
dN/dt	ef	1.11×10^{-1}	–	[1]
	f	1.25×10^{-2}	Day ⁻¹	[6,9,19,40,48]
	p	2.794×10^{-13}	Cells ⁻¹ per day ⁻¹	[1,21,28,30,33,35,39,46]
	p_N	6.68×10^{-2}	Day ⁻¹	[30]
	g_N	2.5036×10^5	IU/l ⁻¹	[1]
	K_N	6.75×10^{-2}	Day ⁻¹	[44]
	δ_N	1.8328	l/mg ⁻¹	[18]
dL/dt	m	9×10^{-3}	Day ⁻¹	[20]
	θ	2.5036×10^{-3}	IU/l ⁻¹	[1,41]
	q	3.422×10^{-10}	Cells ⁻¹ per day ⁻¹	[25,27]
	r_1	2.9077×10^{-11}	Cells ⁻¹ per day ⁻¹	[5,21]
	r_2	5.8467×10^{-13}	Cells ⁻¹ per day ⁻¹	No source
	p_I	2.971	Day ⁻¹	[1,21,28,30,33,35,39,46]
	g_I	2.5036×10^3	IU/l ⁻¹	[1]
	u	4.417×10^{-14}	l ² /cells ⁻² per day ⁻¹	[1,21,28,30,33,35,39,46]
	k	2.5036×10^3	IU/l ⁻¹	[1,41]
	j	1.245×10^{-2}	Day ⁻¹	[27]
	k	2.019×10^7	Cells	[27]
	K_L	4.86×10^{-2}	Day ⁻¹	[44]
	δ_L	1.8328	l/mg ⁻¹	[18]
dC/dt	α/β	2.25×10^{-1}	Cells/l ⁻¹	[1]
	β	6.3×10^{-3}	Day ⁻¹	[9,12,17,19]
	K_C	3.4×10^{-2}	Day ⁻¹	[44]
	δ_C	1.8328	l/mg ⁻¹	[18]
dM/dt	γ	5.199×10^{-1}	Day ⁻¹	[22,47]
dl/dt	μ_l	11.7427	Day ⁻¹	[26]
	ω	7.874×10^{-2}	IU/cells ⁻¹ per day ⁻¹	[1,21,28,30,33,35,39,46]
	ϕ	2.38405×10^{-7}	IU/cells ⁻¹ per day ⁻¹	[1,21,28,30,33,35,39,46]
	ζ	2.5036×10^3	IU/l ⁻¹	[1]
D	d	Not specified	Day ⁻¹	[15]
	l	Not specified	–	[12,13]
	s	Not specified	l ^{-l}	[12,13]

assumption that we have 18×10^6 IU IL-2 per 1.1 mg IL-2 [33]. Finally, L is derived from Pittet *et al.* [39], who indicate that in healthy blood donors, total CD8⁺T cells specific for the Melan-A gene (a tumour-associated antigen in melanoma) constitute approximately 0.0421% of total CD8⁺T cells. The average of all healthy donor values in Table 1 of Pittet *et al.* and Speiser *et al.* [46] show that we can associate the activated CD8⁺T-cell population with those expressing 2B4. Since in Figure 5b of Speiser *et al.* approximately 10% of Melan-A specific T cells express 2B4, we see that 0.00421% of all CD8⁺T cells are expected to be activated and specific for a tumour-associated antigen. Although Melan-A is not always the most heavily expressed tumour-associated-antigen even in melanoma, data from Table 2 in Lee *et al.* [28] suggest that other antigens will result in a similar degree of CD8⁺T-cell activation. This gives the equilibrium value of L when combined with the value for total CD8⁺T cells of 6×10^8 ([21]; p. 751).

The second equilibrium point, we call the *large-tumour equilibrium* and this is given by

$$T=9.8039 \times 10^8, N=2.5 \times 10^8, L=5.268 \times 10^5, C=\frac{\alpha}{\beta}=2.25 \times 10^9, M=0, I=1073, \quad (9)$$

We again define $M=0$ as we are not interested in the effects of chemotherapy. The algebraic expressions for T and C follow from the model, as in the no-tumour equilibrium. Numerical values are again derived below (see the justifications of b in Section 3.2, elf in Section 3.3 and α/β in Section 3.5.) N is derived from Figure 1 in Meropol *et al.* [30], who measure the baseline concentration of NK cells in peripheral blood of breast cancer patients. I is again taken from Orditura *et al.* [35], who measure that serum IL-2 levels were on average $I = 71.69 \text{ pg/ml} = 1173 \text{ IU/l}$ in stage III cancer patients prior to chemotherapy. Note that we use the value for stage III patients to avoid including patients with metastatic cancer, as the model is designed to represent localized malignancy. Finally, L is derived from Lee *et al.* [28] by averaging the percent of CD8 data in Lee's Table 2 among the first five populations, which are activated for an antigen, to arrive at an average of 0.0878% activated CD8⁺T cells specific for one of the melanoma antigens Melan-A/Mart-1 and tyrosinase. Along with the total CD8⁺T-cell value above from Janeway *et al.* [21]; (p. 751), this gives the equilibrium value for L .

3.2 dT/dt : The tumour

$a = 4.31 \times 10^{-1}$ is left unchanged from the de Pillis *et al.* [12] model, as the model is extraordinarily sensitive to a and no data could be found supporting a different value. De Pillis *et al.* [12] derived the parameter from Diefenbach *et al.* [14].

$b = 1.02 \times 10^{-9}$ is also left unchanged from the de Pillis *et al.* [12] model. Both de Pillis *et al.* [13] and de Pillis *et al.* [12] arrived at the same value from Diefenbach *et al.* [14], suggesting that this parameter is well-substantiated. Note that $1/b = 9.8039 \times 10^8$ is the tumour carrying capacity.

$c = 2.9077 \times 10^{-13}$ is based on the approximation that for every NK cell that kills a tumour cell, one NK cell dies. We then let $c = p$, since c is the rate at which NK cells kill tumour cells and p is the rate at which NK cells die from the same process. Note that the value of p is derived in Section 3.3. Although we lack documentation for our approximation, the near equality of p and c in the de Pillis *et al.* [12] model implies that we are not conceptually contradicting previous work. As further substantiation for our value of c , chromium-release assays in Dudley *et al.* [15] and Diefenbach *et al.* [14] suggest that NK cells kill tumour cells at a mass-action rate of $\approx 10^{-7}$ *in vitro*. This is comparable to the value $c = 3.23 \times 10^{-7}$ used in de Pillis *et al.* [13]. However, because NK cells circulate and do not solely exist in the vicinity of the tumour, an *in vitro* value cannot be directly applied to a human model. Instead, we approximate (in agreement with de Pillis *et al.* [12]) that only 1 in 10^6 NK cells interacts with the tumour *in vivo*, which leads to the conclusion that c is on the order of 10^{-13} . The approximation is derived from estimates of 10^8 cells in an average tumour and 10^{14} cells in the human body, so if NK cells distribute themselves evenly over all tissue, only 1 in 10^6 will lie in the tumour. As our interaction assumption and order-of-magnitude derivation agree, the value of c appears reasonable.

$K_T = 0.9$ is left unchanged from the de Pillis *et al.* [12] model, as we found no data supporting a different value. de Pillis *et al.* [12] took it originally from Ref. [37].

$\delta_T = 1.8328$ is taken from Gardner [18]. Table 4 of Gardner lists a value of $\alpha = 1.063 \mu\text{M}^{-1}$ for doxorubicin acting on the primary cell line. Since our medicine kill

Table 4. Simulation results for patient 9, patient 10. Here, x represents the eradication of the tumour and o denotes the survival of the tumour).

Simulation Patient number	$T = 1 \times 10^6$ cells		$T = 1 \times 10^7$ cells		$T = 1 \times 10^8$ cells		$T = 1 \times 10^9$ cells	
	9	10	9	10	9	10	9	10
No treatment	x	x	o	o	o	o	o	o
Chemotherapy	x	x	x	x	x	x	o	o
Immunotherapy	x	x	x	o	o	o	o	o
Chemo-immuno	x	x	x	x	x	o	o	o

term reflects the dynamics suggested in Gardner, we use Gardner’s value of a converted to units of l/mg. Taking the molar mass of doxorubicin HCl as 579.99 g/mol [43], we arrive at our value for δ_T as follows:

$$\begin{aligned} \delta_T &= 1.063 \text{ l}/\mu\text{mol} \left(\frac{1 \times 10^6 \mu\text{mol}}{1 \text{ mol}} \right) \left(\frac{1 \text{ mol}}{579.99 \text{ g doxorubicin}} \right) \left(\frac{1 \text{ g}}{1000 \text{ mg}} \right) \\ &= 1.83281/\text{mg}. \end{aligned}$$

3.3 dN/dt : The natural killer cells

$elf = 1.11 \times 10^{-1}$ is equal to the ratio N/C at equilibrium if we ignore the small effect of IL-2 on NK proliferation in the absence of exogenous supplementation. Since Abbas *et al.* ([1]; p. 19) indicate that NK cells make up approximately 10% of total circulating lymphocytes in the absence of a tumour, and the number of activated $CD8^+T$ cells L is several orders of magnitude smaller than N in healthy blood donors and thus negligible (see the no-tumour equilibrium condition (8)), we can approximate $elf = 1/9 \approx 1.11 \times 10^{-1}$. Note that C here measures the number of total lymphocytes that are neither activated $CD8^+T$ cells nor NK cells.

$f = 1.25 \times 10^{-2}$ was found by metabolic scaling. The average mass of an adult human male is 77 kg and the average mass for an adult male rhesus monkey is 11.9 kg [40,48]. From Gillooly *et al.* [19], we see that mass-specific metabolic rate B scales as:

$$B/M \propto M^{-1/4},$$

where M is mass. We do recognize that there is consideration for different scaling behaviour depending on the location of cells in the body. However, Gillooly *et al.* [19] explain that when the masses of two organisms differ significantly, the scaling law is obeyed with good

Animal	Mass (kg)	$M^{-1/4}$ ($\text{kg}^{-1/4}$)
Human	77	0.3376
Rhesus monkey	11.9	0.5384

precision. We have

We assume that f , corresponding to the turnover rate of NK cells, is proportional to mass-specific metabolic rate. Since we have $f_{\text{monkey}} = 2 \times 10^{-2}$ for a rhesus monkey taken from de Boer *et al.* [9], we have:

$$f = \Gamma(B/M) = \Gamma' M^{-1/4},$$

where Γ and Γ' are constants, and the second equality follows from the aforementioned proportionality. Now:

$$\Gamma' = \frac{f_{\text{monkey}}}{M_{\text{monkey}}^{-1/4}} = 0.0371,$$

from the data for the rhesus monkey. Using this to find f for a human, we have:

$$f = \Gamma' M_{\text{human}}^{-1/4} = 1.25 \times 10^{-2},$$

for an average human.

$p = 2.794 \times 10^{-13}$ is obtained by considering that at the large-tumour equilibrium and in the absence of medicine, we have

$$0 = \frac{dN}{dt} = f \left(\frac{e}{f} C - N \right) - pNT + \frac{p_N NI}{g_N + I},$$

The term $((e/f)C - N)$ is zero because we make the assumption in this case that at equilibrium $ef = N/C$. We then have:

$$p = \frac{p_N I}{T(g_N + I)}.$$

Using the values of p_N and g_N calculated below and the equilibrium values from Equation (9), we arrive at our value for p .

$g_N = 2.5036 \times 10^5$ is derived from Abbas *et al.* ([1]; p. 265), where we see the concentration of IL-2 required for half-maximal binding of cells expressing the IL-2R $\beta\gamma_c$ receptor complex is 10^{-9} mol/l, as opposed to 10^{-11} mol/l for cells expressing the IL-2R $\alpha\beta\gamma_c$ receptor complex. Since NK cells express the former receptor exclusively, we arrive at our value for g_N by using 15,300 Da (15,300 g/mol) as the molecular mass of IL-2 and employing the conversion factor of 18×10^6 IU IL-2 per 1.1 mg IL-2 to convert molar concentration to IU/l [1,33]. We therefore have:

$$g_N = \left(\frac{1 \times 10^{-9} \text{ mol}}{11} \right) \left(\frac{15,300 \text{ g}}{1 \text{ mol}} \right) \left(\frac{1000 \text{ mg}}{1 \text{ g}} \right) \left(\frac{1.8 \times 10^7 \text{ IU}}{1.1 \text{ mg}} \right) = 2.5036 \text{ IU/l}.$$

$p_N = 6.68 \times 10^{-2}$ is taken from data in Meropol *et al.* [30] measuring NK cell proliferation in response to IL-2 in the absence of a tumour. Note that p_N measures how effectively NK cells are stimulated by IL-2 and is independent of the presence of a tumour. We assume that the peak NK cell count $N = 2.3 \times 10^9$ in Figure 3 of Meropol *et al.* [30] corresponds to the equilibrium value of N subject to the peak value of IL-2 $I = 200$ pmol/l $= 5.0073 \times 10^4$ IU from Figure 4 of Meropol *et al.* [30]. Assuming now that we have exogenous IL-2 supplementation, we allow for a non-negligible effect of IL-2 on NK cell proliferation. Thus, the term $((e/f)C - N)$ in (2) is now assumed to be non-zero. Additionally, we assume pNT is small, as in the absence of a tumour, and we have:

$$0 = \frac{dN}{dt} = f \left(\frac{e}{f} C - N \right) + \frac{p_N NI}{g_N + I},$$

which gives

$$p_N = \frac{f \left(N - \frac{e}{f} C \right) (g_N + I)}{NI}.$$

We then use $C = 2.25 \times 10^9$ as our equilibrium circulating lymphocyte concentration from the no-tumour equilibrium (8) and the values of N and I above to calculate p_N .

$K_N = 6.75 \times 10^{-2}$ is derived from linearly scaling K_C by the ratio of cell metabolic rates. More precisely, we let:

$$K_N = \frac{f}{\beta} K_C.$$

From the observation in de Pillis *et al.* [12], we know that cells with a faster metabolic rate are killed more effectively by doxorubicin. Lacking evidence to the contrary, we assume this relationship is linear.

$\delta_N = \delta_T = 1.8328$ by assuming that similar concentrations of doxorubicin are necessary to affect all cell types, even though the drug has differential efficacy depending on the metabolic rate of the cell.

3.4 dL/dt : The $CD8^+$ T cells

$m = 9 \times 10^{-3}$ is from Hellerstein *et al.* [20], who put the half-life of $CD8^+$ cells at 77 days in healthy donors. Assuming exponential decay and using $m = m \times t_{1/2} = \ln 2$, we arrive at our value for m .

$\theta = 2.5036 \times 10^3$ was derived from Abbas *et al.* [1] based on the existence of the $IL-2R\alpha\beta\gamma_c$ receptor on $CD8^+$ T cells. Consequently, the concentration needed for half-maximal $IL-2$ binding is 10^{-11} mol/l, which works out to 2.5036×10^3 IU/l, as in the derivation of g_N .

$q = 3.422 \times 10^{-10}$ was taken from Kuznetsov *et al.* [27] as we are unable to find kinetics data on activated $CD8^+$ T-cell–tumour interaction. It must be recognized that Kuznetsov *et al.* [27] used mouse data and modelled the effector cell population, as opposed to the $CD8^+$ T-cell population, but we found no other data suggesting values for q, j and k . In support of our value of q however, we expect q to be approximately three orders of magnitude less than p , due to the relative magnitudes of L and N (based on the two sets of equilibrium values (8), (9)) and this is indeed the case.

$r_1 = 100 \times c = 2.9077 \times 10^{-11}$ is derived from the approximation that each lysed tumour cell, through antigen-presenting pathways, can activate 50 naive $CD8^+$ T cells per day. This figure is adapted from Avigan *et al.* [5], who note that a single dendritic cell can stimulate 100–3000 T cells over the course of its life in the presence of an antigen. Rudel *et al.* [42] indicate that the turnover rate of at least one type of dendritic cell is 10 days, suggesting that a dendritic cell may stimulate 10–300 T cells per day. We choose the figure of 100 T cells/l per day, since neither an average nor a standard deviation is given in Avigan *et al.* [5]. Even at this level, the parameter r_1 turns out not to have an enormous impact relative to the other model parameters.

$r_2 = 5.8467 \times 10^{-13}$ is chosen to obtain a model consistent with expectations, much in the same way as de Pillis *et al.* chose the value of r_2 in their model. There are very limited data on $CD4^+$ T-cell (the primary constituent of C) activation of $CD8^+$ T cells, and we found no research measuring the kinetics.

$u = 4.417 \times 10^{-14}$ is derived by solving a system of equations designed to produce reasonable equilibrium behaviour. The two equilibrium conditions (8) and (9) combined with the known dL/dt parameter values in this section fix all variables in dL/dt other than p_I and u . We thus set $dL/dt = 0$, insert the two sets of equilibrium values into Equation (3) along with the values of all parameters except for u and p_I and thereby obtain two equations in u and p_I . Solving these equations numerically gives us our solution.

$\kappa = 2.5036 \times 10^3$ was obtained from Abbas *et al.* [1] in the same way as θ . Refaeli *et al.* [41] observe that upon removal of the α IL-2 receptor chain, CD8⁺T cells fail to self-regulate. This affirms that κ should correspond to the disassociation constant for the IL-2R $\alpha\beta\gamma_c$ receptor.

$p_I = 2.971$ is taken from the solution to the system in u and p_I above.

$g_I = 2.5036 \times 10^3$ is derived from Abbas *et al.* [1] in the same way as θ and κ .

$j = 1.245 \times 10^{-1}$ is taken from Kuznetsov *et al.* [27] for lack of data in humans.

$k = 2.019 \times 10^7$ is taken from Kuznetsov *et al.* [27] for lack of data in humans.

$k_L = 0.0486$ is derived from the same linear metabolic scaling used to derive K_N from K_C . Thus, we let:

$$K_L = \frac{m}{\beta} K_C,$$

and thereby find K_L .

$\delta_L = 1.8328$ is approximated under the assumption of equality with δ_T as in the derivation of δ_N .

3.5 dC/dt : The circulating lymphocytes

$\alpha/\beta = C = 2.5 \times 10^9$ follows as under normal healthy conditions, $dC/dt = 0$ and no chemotherapy medicine is present. We take the average value of circulating lymphocytes to be 2.5×10^9 cells/l ([1]; p. 17). However, we factor out both NK, which cells make up 10% of circulating lymphocytes in a healthy human, and activated CD8⁺T cells, which constitute a negligible fraction of circulating lymphocytes as noted in the derivation of f , due to their plastic nature [1]. Consequently, we have:

$$\frac{\alpha}{\beta} = (2.5 \times 10^9)(0.9) = 2.25 \times 10^9.$$

$\beta = 6.3 \times 10^{-3}$ is obtained by taking the 1% turnover rate of CD4⁺T cells (which are the primary constituent of the population measured by C) in rhesus monkeys cited in Boer *et al.* [9] and applying metabolic scaling. (See the explanation of f .)

$K_C = 0.034$ is derived from the observation that the median white blood cell count after doxorubicin treatment for several weeks using exactly our treatment protocol was 1.6×10^3 cells/ μ l = 1.6×10^9 cells/l [44]. If we assume that in these patients we still have the relationship $N = (1/10)C$, then this white blood cell count (which includes all circulating lymphocytes) should correspond to $C = (9/10)(1.6 \times 10^9) = 1.44 \times 10^9$. By repeatedly running ODE simulations of the dC/dt ODE, which is independent of all but M , with the no-tumour equilibrium data (8) and chemotherapy turned on, we found that $K_C = 0.155$ produced a nadir value of $C = 1.447 \times 10^9$ as desired.

$\delta_C = 1.8328$ is approximated under the assumption of equality with δ_T .

3.6 dM/dt : The chemotherapy

$\gamma = \ln 2/1.3332$ days = 0.5199 is derived from the assumption of exponential decay. The tissue (as opposed to blood, from which the drug is eliminated rapidly) elimination half-life of doxorubicin, the chemotherapy medicine on which the de Pillis *et al.* [12] model is based, is approximately 32 h or 1.3332 days [22,47].

3.7 dI/dt : The IL-2

$\mu_I = \ln 2 / 5.90 \times 10^{-2}$ days = 11.7427 days⁻¹ is again derived from assumption of exponential decay. The half-life of serum IL-2 is biphasic with a tissue elimination half-life of $t_{1/2} = 85$ min [26]. Our value follows after converting to days.

$\omega = 7.874 \times 10^{-2}$ was found by a similar procedure to that used to find u . Using the equilibrium values (8), (9) and the known dI/dt parameters, we found ω and ϕ by solving a system of equations generated by setting $dI/dt = 0$ and inserting both sets of equilibrium conditions.

$\phi = 2.38405 \times 10^{-7}$ was found as part of the solution to the system created to find ω .

$\zeta = g_I = 2.5036 \times 10^3$, as the term comprising ζ pertains to CD8⁺T-cell IL-2 synthesis induced by IL-2, which depends on the IL-2R $\alpha\beta\gamma_c$ receptor, as in θ .

3.8 D : The CD8⁺T-cell cytotoxicity parameter

We have three patient-specific parameters in the model. These are d , l and s , the parameters in D ; they are some of the few parameters from de Pillis *et al.* that vary between patients 9 and 10. Simulations also show that the model is highly sensitive to the value of all three parameters. We therefore choose not to specify d , l and s and instead vary them as we run our simulations.

4. Results

In our simulations, we vary the initial tumour size, but keep all other initial state values fixed at the large-tumour equilibrium (9) values derived in Section 3.1. We restate them here as our initial conditions:

$$N_0 = 2.5 \times 10^8, \quad L_0 = 5.268 \times 10^5, \quad C = 2.25 \times 10^9, \quad M_0 = 0, \quad I_0 = 1073. \quad (10)$$

We also constructed a basic treatment protocol for each of v_L , v_M and v_I and ran ODE simulations with varying initial tumour sizes and combinations of treatments.

For chemotherapy, we follow the recommended dosage suggested by the manufacturers of the drug Adria (doxorubicin HCl [43]). The suggested procedure entails a single dose of 60–75 mg/m² once every 21 days. We approximate an average human male to have surface area of 1.9 m², as given in Ref. [31], and we use the upper end of the dosing range to arrive at 142.5 mg doxorubicin every 21 days. Note that we model each half-hour infusion by setting v_M to be constant and elevated for a full day. According to Ref. [22], doxorubicin has an extremely rapid distribution half-life and exits the bloodstream within minutes. Thus to get the concentration in the bloodstream (and in fact in all tissues, assuming uniform distribution), we use the figure of 59.71 average body volume for a man from Table 1 in Sendroy *et al.* [45] to get $v_M = 2.3869$ mg/l per day.

Dudley *et al.* [15] in their Table 1 compile a set of T-cell dosing protocols for individual patients. The number of CD8⁺T cells injected into each patient ranges from 2.2×10^{10} to 12.2×10^{10} . The average of the values in Dudley's Table 1 is 7.8×10^{10} CD8⁺T cells per day. To convert the value from an absolute population to a resulting blood concentration, we divide by 4.41 and set $v_L = 1.77 \times 10^{10}$ CD8⁺T cells/l per day given once [6]. We model the single infusion by increasing v_L to this value for a day.

Also in Dudley's Table 1 [15], the authors note that they inject 7.2×10^5 IU/kg IL-2 every 8 h (0.33 days) after the T-cell infusion for an average of 9 total IL-2 treatments. However, according to Ref. [26], IL-2 also has a very rapid distribution half-life. Consequently, as with v_M , we assume uniform distribution over all tissues. Using the average adult male human weight of 77 kg and again assuming 59.71 of body volume,

we model this dosing regimen as 2.7859×10^6 IU IL-2/l per day for three days, spread evenly over the course of each day [40,48]. Note that immunotherapy refers to the combination of CD8⁺T-cell infusion with the above IL-2 treatment.

Only the CD8⁺T-cell infusion treatment need be modified, and we simply convert it from an absolute population to a resulting blood concentration by again dividing by 4.41 [6]. We obtain:

$$v_L = 1.77 \times 10^{10}, \quad v_M = 2.3869, \quad v_I = 2.7859 \times 10^6. \tag{11}$$

Because we have three highly patient-specific parameters, as noted in Section 3.8, we separate our results for patient 9 and patient 10 from de Pillis *et al.* [12]. Note, however, that because the de Pillis *et al.* [12] model uses the total population of L as opposed to the blood concentration, we must divide s by V^l , where $V = 4.41$ is again the average human blood volume [6]. The results are stated below:

	d	l	s	
Patient 9	2.34	2.09	3.8×10^{-3}	(12)
Patient 10	1.88	1.81	3.5×10^{-2} ,	

We ran all simulations for 200 days, as it was experimentally determined that all populations either reached equilibrium or became stably periodic within this time period. The results with a variety of initial tumour sizes are compiled in Table 4.

We may interpret the parameters d , l and s loosely as the strength or efficiency of the patient’s immune system; these parameters correspond to the efficacy at which CD8⁺T cells kill cancer cells. We then see from our Table 4 that patient 10 has a weaker immune system than patient 9. Indeed, the results of pure chemotherapy are essentially identical between the 2 patients, but the success of immunotherapy and mixed treatment are superior in patient 9. This is to be expected, as a patient with more efficient immune-tumour dynamics would be expected to benefit more from a boost to the immune system. This may suggest that an assessment of innate immune strength is in order before determining a treatment course; patients with low CD8⁺T-cell efficacy may not benefit from immunotherapy and might be optimally placed on chemotherapy alone, whereas other patients might benefit enormously from combined therapy.

We highlight a few simulations of particular interest. Figure 1 shows the results of our model with no therapy and an initial tumour size of $T_0 = 1 \times 10^7$ cells. The immune system is not able to kill the tumour unaided and the tumour grows to its large-tumour equilibrium value. CD8⁺T cells and NK cells remain stable at their expected equilibrium values from (9). Similarly, as intended with the introduction of endogenous IL-2 synthesis, serum IL-2 ultimately remains at its expected equilibrium value.

In Figure 2, we keep the initial tumour size at $T_0 = 1 \times 10^7$ cells and initiate chemotherapy; the tumour is rapidly destroyed. This is a reasonable outcome with chemotherapy treatment on a relatively small tumour.

Finally, Figure 3 shows the results of combined therapy on a tumour of initial size $T_0 = 1 \times 10^8$ cells. The tumour is eliminated under these conditions. We see only a slight reduction in activated CD8⁺T and NK cells concentrations as expected [23].

The numerics provide strong evidence that this system with these parameter values has at least two stable equilibrium points: one stable zero tumour equilibrium, and one stable large tumour equilibrium. Further analysis would be needed to confirm this, as well as to determine how the number and stability properties of the equilibrium points are affected by parameter changes.

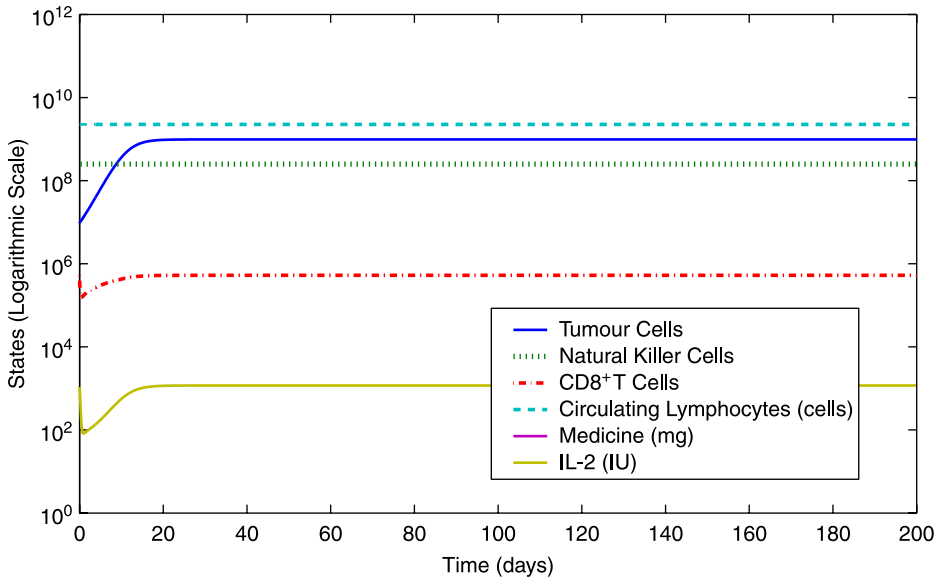


Figure 1. Model simulation: $T_0 = 1 \times 10^7$ cells, simulation with initial conditions (10) and $T_0 = 1 \times 10^7$ cells. The patient's unaided immune system is not able to destroy the tumour. No changes in circulating lymphocyte or NK cell concentrations are seen, as expected.

5. Numerical sensitivity analysis

A numerical parameter sensitivity analysis can highlight those model parameters that have the greatest effect on model outcome. A standard approach to performing this analysis is to fix all parameter values but one, and then to increase and decrease that one parameter by a certain

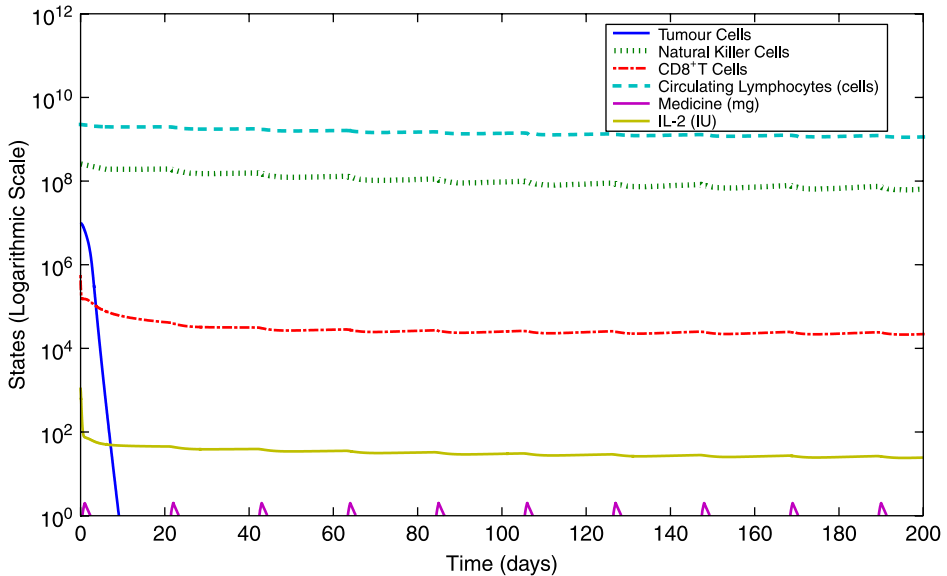


Figure 2. Model simulation $T_0 = 1 \times 10^7$ cells with chemotherapy, simulation with initial conditions (10), chemotherapy treatment (11) and $T_0 = 1 \times 10^7$ cells. Adding chemotherapy successfully kills the tumour, as expected for a relatively small initial tumour size.

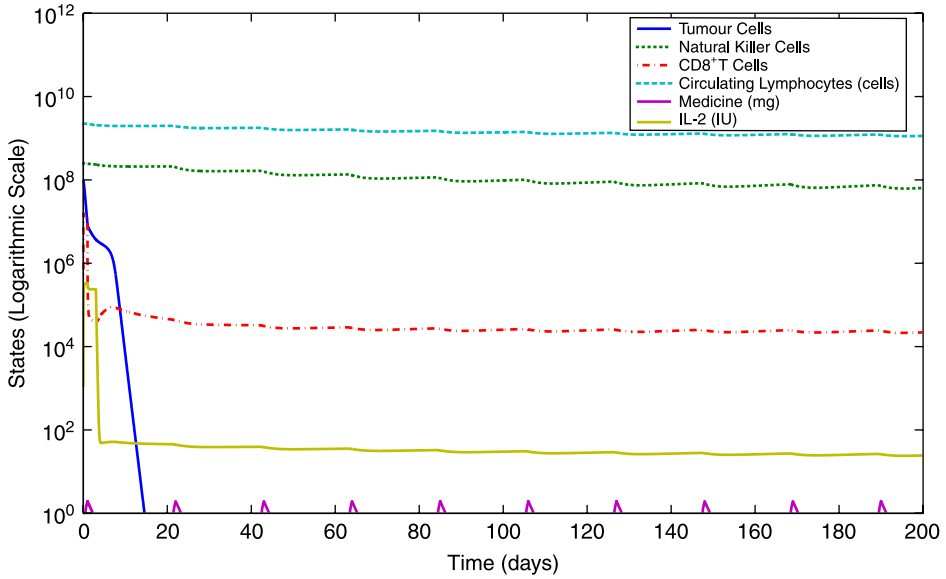


Figure 3. Model simulation $T_0 = 1 \times 10^8$ cells with chemotherapy and immunotherapy, simulation with initial conditions (10), chemotherapy and immunotherapy treatment (11) and $T_0 = 1 \times 10^8$ cells. The tumour is rapidly eliminated. Activated CD8⁺T and NK cells drop slightly but still in agreement with [23].

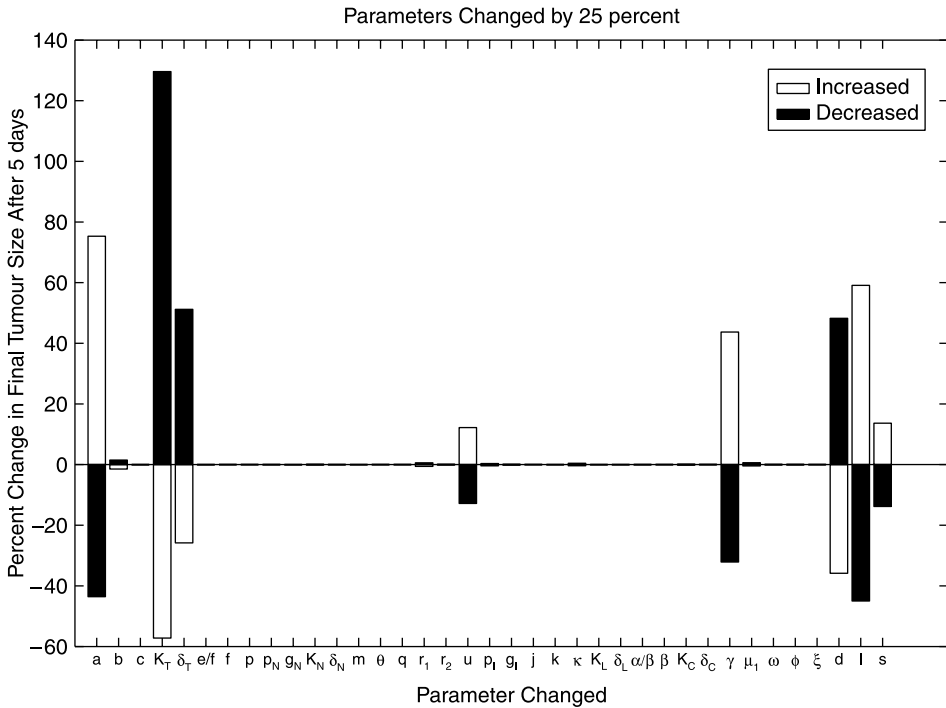


Figure 4. Numerical sensitivity analysis. Depicted is the effect of a 25% parameter change on final tumour size after 10 days. Initial conditions are as in Equation (10), with initial number of tumour cells $T_0 = 1 \times 10^8$. Patient 10 parameters were used.

percentage, and examine the effect on the model endpoints. In Figure 4, we plot the percent change in tumour size from day zero to day five as a result of changing each of the model parameters by 25% in both directions. The fixed parameter values are taken from Table 3.

We note that although the model does have a relatively large number of parameters, it is clear that the model is significantly more sensitive to the changes in a few parameters than to the remaining parameters. It is not surprising, for example, that final tumour size is highly sensitive to the intrinsic tumour growth rate a and to the strength of the chemotherapy action against the tumour, as represented by K_T and δ_T . The model is sensitive to u since CD8⁺T cells are the primary killers of tumour cells other than chemotherapy. Modifying u dramatically changes how many CD8⁺T cells are created due to IL-2 in a short period of time. Parameter γ represents the rate of decay of the chemotherapy drug in the system. We therefore see sensitivity to γ , since this is related to the length of time the chemotherapy has to act against the tumour. We also see significant sensitivity to the values of d , l and s . These parameters are all related to the effectiveness of the CD8⁺T cells in stemming the growth of the tumour. Interestingly, it may be theoretically possible to determine these parameters through fits to patient-specific assay data, as was done in de Pillis *et al.* [13].

6. Discussion

We have updated the de Pillis *et al.* model [12] by incorporating the latest research on baseline NK and activated CD8⁺T-cell concentrations in both healthy donors and cancer patients. We have also included endogenous IL-2 production, added IL-2-stimulated NK cell proliferation and refined the IL-2-dependent regulation of activated CD8⁺T cells. The results of our model align with recent data measuring baseline blood concentrations of several immune populations and, in particular, of IL-2. Moreover, we have carefully updated several parameter values with data from *in vivo* and *in vitro* research on turnover rates and mass-action kill rates. For the remaining parameters, we solved for the needed values using numerical equilibrium point information.

The results obtained from patients with different degrees of CD8⁺T-cell efficacy display insight into the potential success of immunotherapy. If individual CD8⁺T-cell tumour lysis data can be obtained, it may be possible to determine the potential use of immunotherapy as an adjunct to chemotherapy. Our updated model indicates that the more effectively CD8⁺T cells taken from peripheral blood kill tumour cells, the more useful immunotherapy may be in conjunction with chemotherapy. Conversely, in patients with low immune efficacy, immunotherapy may be of relatively little help in eliminating cancerous tissue, as was seen in patient 10 from de Pillis *et al.* [12].

Further extensions to our model may be possible when more data become available on mass-action kill rates of NK and tumour antigen-specific CD8⁺T cells, as well as when more precise estimates of immune cell recruitment rates can be obtained. Moreover, a next step may be to further fractionate the circulating lymphocytes and track the helper or memory CD4⁺T-cell and dendritic cell populations, as both are intricately involved in activation and synthesis of CD8⁺T cells.

Acknowledgements

This work was supported in part by generous funding from the W. M. Keck Foundation through the Harvey Mudd College Center for Quantitative Life Sciences as well as by the National Science Foundation Grant Number DMS-0414011, 'Mathematical Modeling of the Chemotherapy, Immunotherapy and Vaccine Therapy of Cancer' for the students and Professors de Pillis, Gu and

Fister. Any opinions, findings and conclusions or recommendations expressed in this material are those of the authors and do not necessarily reflect the views of the National Science Foundation.

Note

1. This work was supported by the National Science Foundation under grant NSF-DMS-041-4011.

References

- [1] A.K. Abbas and A.H. Lichtman, *Cellular and Molecular Immunology*, 5th ed., Elsevier Saunders, St. Louis, MO, 2005.
- [2] J.A. Adam and N. Bellomo, *Survey of Models for Tumor-Immune System Dynamics*, Birkhauser, Boston, 1997.
- [3] J.C. Arciero, T.L. Jackson, and D.E. Kirschner, *Mathematical model of tumor-immune evasion and siRNA treatment*, Discrete Contin. Dyn. Syst. Ser. B 4 (2004), pp. 39–58.
- [4] B. Asquith, C. Debaq, A. Florins, N. Gillet, T. Sanchez-Alcaraz, A. Mosley, and L. Willems, *Quantifying lymphocyte kinetics in vivo using carboxyfluorescein diacetate succinimidyl ester (CFSE)*, Proc. R. Soc. B 273 (2006), pp. 1165–1171.
- [5] D. Avigan, *Dendritic cells: Development, function and potential use for cancer immunotherapy*, Blood Rev. 13 (1999), pp. 51–64.
- [6] J.R. Cameron, J.G. Skofronick, and R.M. Grant, *Physics of the Body*, Medical Physics Publishing, Madison, WI, 1999.
- [7] M. Chaplain and A. Matzavinos, *Mathematical modeling of spatio-temporal phenomena in tumour immunology*, Tutor. Math. Biosci. III (2006), pp. 131–183.
- [8] R.J. De Boer, P. Hogeweg, H.F.J. Dullens, R.A. De Weger, and W. DenOtter, *Macrophage *t* lymphocyte interactions in the anti-tumor immune response: A mathematical model*, J. Immunol. 134 (1985), pp. 2748–2758.
- [9] R.J. De Boer, H. Mohri, D.D. Ho, and A.S. Perelson, *Turnover rates of B cells, T cells, and NK cells in simian immunodeficiency virus-infected and uninfected rhesus macaques*, J. Immunol. 170 (2003), pp. 2479–2487.
- [10] S. De Lillo, M.C. Salvatori, and N. Bellomo, *Mathematical tools of the kinetic theory of active particles with some reasoning on the modelling progression and heterogeneity*, Math. Comput. Model. 45 (2007), pp. 564–578.
- [11] A. d’Onofrio, *Tumor evasion from immune control: Strategies of a miss to become a mass*, Chaos Solitons Fractals 31 (2007), pp. 261–268.
- [12] L.G. de Pillis, W. Gu, and A.E. Radunskaya, *Mixed immunotherapy and chemotherapy of tumors: Modeling, applications, and biological interpretations*, J. Theor. Biol. 238 (2006), pp. 841–862.
- [13] L.G. de Pillis, A.E. Radunskaya, and C.L. Wiseman, *A validated mathematical model of cell-mediated immune response to tumor growth*, Cancer Res. 65 (2005), pp. 7950–7958.
- [14] A. Diefenbach, E.R. Jensen, A.M. Jamieson, and D.H. Raulet, *Rae1 and H60 ligands of the NKG2D receptor stimulate tumor immunity*, Nature 413 (2001), pp. 165–171.
- [15] M.E. Dudley et al., *Cancer regression and autoimmunity in patients after clonal repopulation with antitumor lymphocytes*, Science 298 (2002), pp. 850–854.
- [16] J. Dunne, S. Lynch, C. O’Farrelly, S. Todryk, J.E. Hegarty, C. Feighery, and D.G. Doherty, *Selective expansion and partial activation of human NK cells and NK receptor-positive T cells by IL-2 and IL-15*, J. Immunol. 167 (2001), pp. 3129–3138.
- [17] E.J. Freireich, E.A. Gehan, D.P. Rall, L.H. Schmidt, and H.E. Skipper, *Quantitative comparison of toxicity of anticancer agents in mouse, rat, hamster, dog, monkey and man*, Cancer Chemother. Rep. 50 (1966), pp. 219–244.
- [18] S.N. Gardner, *A mechanistic, predictive model of dose-response curves for cell cycle and phase-specific and -nonspecific drugs*, Cancer Res. 60 (2000), pp. 1417–1425.
- [19] J.F. Gillooly, J.H. Brown, G.B. West, V.M. Savage, and E.L. Charnov, *Effects of size and temperature on metabolic rate*, Science 293 (2001), pp. 2248–2251.
- [20] M. Hellerstein et al., *Directly measured kinetics of circulating T lymphocytes in normal and HIV-1-infected humans*, Nat. Med. 5 (1999), pp. 83–89.
- [21] C.A. Janeway, P. Travers, Jr., M. Walport, and M.J. Sclomchik, *Immunobiology*, Garland Science Publishing, London, 2005.

- [22] M. Joerger, A.D.R. Huitema, P.L. Meenhorst, J.H.M. Schellens, and J.H. Beijnen, *Pharmacokinetics of low-dose doxorubicin and metabolites in patients with AIDS-related kaposi sarcoma*, *Cancer Chemother. Pharmacol.* 55 (2005), pp. 488–496.
- [23] V. Jurisic, G. Konevic, O. Markovic, and M. Colovic, *Clinic stage-depending decrease of NK cell activity in multiple myeloma patients*, *Med. Oncol.* 24 (2007), pp. 312–317.
- [24] D. Kirschner and J.C. Panetta, *Modeling immunotherapy of the tumor–immune interaction*, *J. Math. Biol.* 37 (1998), pp. 235–252.
- [25] G. Konjevic and I. Spuzic, *Stage dependence of NK cell activity and its modulation by interleukin 2 in patients with breast cancer*, *Neoplasma* 40 (1993), pp. 81–85.
- [26] M.W. Konrad, G. Hemstreet, E.M. Hersh, P.W. Mansell, R. Mertelsmann, J.E. Kolitz, and E.C. Bradley, *Pharmacokinetics of recombinant interleukin 2 in humans*, *Cancer Res.* 50 (1990), pp. 2009–2017.
- [27] V.A. Kuznetsov, I.A. Makalkin, M.A. Taylor, and A.S. Perelson, *Nonlinear dynamics of immunogenic tumors: Parameter estimation and global bifurcation analysis*, *Bull. Math. Biol.* 56 (1994), pp. 295–321.
- [28] P.P. Lee et al., *Characterization of circulating T cells specific for tumor-associated antigens in melanoma patients*, *Nat. Med.* 5 (1999), pp. 677–685.
- [29] D.G. Mallet and L.G. De Pillis, *A cellular automata model of tumor–immune system interactions*, *J. Theor. Biol.* 239 (2006), pp. 334–350.
- [30] N.J. Meropol, G.M. Barresi, T.A. Fehniger, J. Hitt, M. Franklin, and M.A. Galigiuri, *Evaluation of natural killer cell expansion and activation in vivo with daily subcutaneous low-dose interleukin-2 plus periodic intermediate-dose pulsing*, *Cancer Immunol. Immunother.* 46 (1998), pp. 318S–326S.
- [31] R.D. Mosteller, *Simplified calculation of body-surface area*, *N. Engl. J. Med.* 317 (1987), p. 1098.
- [32] B. Nelson, *IL-2, regulatory T-cells, and tolerance*, *J. Immunol.* 172 (2004), pp. 3983–3988.
- [33] Novartis Pharmaceuticals *Proleukin (aldesleukin): Pharmacology and indications*, January 2007. <http://www.proleukin.com/hcp/tools/pi-pharmacology.jsp>
- [34] A.S. Novozhilov, F.S. Berezovskaya, E.V. Koonin, and G.P. Karev, *Mathematical modeling of tumor therapy with oncolytic viruses: Regimes with complete tumor elimination within the framework of deterministic models*, *Biol. Direct* 1(6) (2006), pp. 1–18.
- [35] M. Orditura, C. Romano, F. De Vita, G. Galizia, E. Lieto, S. Infusino, G. De Cataldis, and G. Catalano, *Behaviour of interleukin-2 serum levels in advanced non-small-cell lung cancer patients: Relationship with response to therapy and survival*, *Cancer Immunol. Immunother.* 49 (2000), pp. 530–536.
- [36] M.R. Owen, H.M. Byrne, and C.E. Lewis, *Mathematical modelling of the use of macrophages as vehicles for drug delivery to hypoxic tumour sites*, *J. Theor. Biol.* 226 (2004), pp. 377–391.
- [37] M.C. Perry, *The Chemotherapy Source Book*, 3rd ed., Lippincott Williams and Wilkins, Philadelphia, PA, 2001.
- [38] B. Piccoli and F. Castiglione, *Optimal vaccine scheduling in cancer immunotherapy*, *Phys. A* 370 (2006), pp. 672–680.
- [39] M.J. Pittet, D. Valmori, P.R. Dunbar, D.E. Speiser, D. Liénard, F. Lejeune, K. Fleischhauer, V. Cerundolo, J.C. Cerottini, and P. Romero, *High frequencies of naive melan-a/MART-1-specific CD8 + T cells in a large proportion of human histocompatibility leukocyte antigen (HLA)-A2 individuals*, *J. Exp. Med.* 190 (1999), pp. 705–715.
- [40] A. Raman, R.J. Colman, Y. Cheng, J.W. Kemnitz, S.T. Baum, R. Weindruch, and D.A. Schoeller, *Reference body composition in adult rhesus monkeys: Glucoregulatory and anthropometric indices*, *J. Gerontol.* 60A (2005), pp. 1518–1524.
- [41] Y. Refaelli, L.V. Parijs, C.A. London, J. Tschopp, and A. Abbas, *Biochemical mechanisms of IL-2-regulated fas-mediated T cell apoptosis*, *Immunity* 8 (1998), pp. 616–623.
- [42] C. Ruedl, P. Koebel, M. Bachmann, M. Hess, and K. Karjalainen, *Antatomical origin of dendritic cells determines their life span in peripheral lymph nodes*, *J. Immunol.* 165 (2000), pp. 4910–4916.
- [43] RxList Inc. *Adria (doxorubicin hydrochloride) drug indications and dosage*, January 2007. http://www.rxlist.com/cgi/generic/adriamycin_ids.htm
- [44] G.K. Schwartz and E.S. Casper, *A phase II trial of doxorubicin HCL liposome injection in patients with advanced pancreatic adenocarcinoma*, *Invest. New Drugs* 13 (1995), pp. 77–82.
- [45] J. Sendroy, Jr., and H.A. Collison, *Determination of human body volume from height and weight*, *J. Appl. Physiol.* 21 (1966), pp. 167–172.

- [46] D.E. Speiser et al., *The activatory receptor 2B4 is expressed in vivo by human CD8 + effector alpha beta T cells*, J. Immunol. 167 (2001), pp. 6165–6170.
- [47] J. Wihlm, J.M. Limacher, D. Levegue, B. Duclos, P. Dufour, J.P. Bergerat, and G. Methlin, *Phar-macokinetic profile of high-dose doxorubicin administered during a 6 h intravenous infusion in breast cancer patients*, Bull. Cancer 84 (1997), pp. 603–608.
- [48] D.F. Williamson, *Descriptive epidemiology of body weight and weight change in US adults*, Ann. Intern. Med. 119 (1993), pp. 646–649.